

See discussions, stats, and author profiles for this publication at: <https://www.researchgate.net/publication/10617976>

Kinetics and Thermodynamics of H• Transfer from $(\eta^5\text{-C}_5\text{R}_5)\text{Cr}(\text{CO})_3\text{H}$ (R = Ph, Me, H) to Methyl Methacrylate and Styrene

ARTICLE in JOURNAL OF THE AMERICAN CHEMICAL SOCIETY · SEPTEMBER 2003

Impact Factor: 12.11 · DOI: 10.1021/ja034927l · Source: PubMed

CITATIONS

42

READS

26

7 AUTHORS, INCLUDING:



Elizabeth T Papish

University of Alabama

36 PUBLICATIONS 487 CITATIONS

SEE PROFILE



Jack R. Norton

Columbia University

181 PUBLICATIONS 5,162 CITATIONS

SEE PROFILE



Mu-Hyun Baik

Korea Advanced Institute of Science and Tec...

115 PUBLICATIONS 3,303 CITATIONS

SEE PROFILE

Kinetics and Thermodynamics of H• Transfer from (η^5 -C₅R₅)Cr(CO)₃H (R = Ph, Me, H) to Methyl Methacrylate and Styrene

Lihao Tang,[†] Elizabeth T. Papish,[†] Graham P. Abramo,[†] Jack R. Norton,^{*,†}
Mu-Hyun Baik,[†] Richard A. Friesner,[†] and Anthony Rappé[‡]

Contribution from the Departments of Chemistry, Columbia University, 3000 Broadway,
New York, New York 10027, and Colorado State University, Fort Collins, Colorado 80523

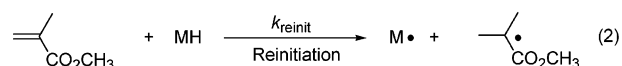
Received February 28, 2003; E-mail: jnorton@chem.columbia.edu

Abstract: The rates of H/D exchange have been measured between (a) the activated olefins methyl methacrylate-*d*₈ and styrene-*d*₈, and (b) the Cr hydrides (η^5 -C₅Ph₅)Cr(CO)₃H (**2a**), (η^5 -C₅Me₅)Cr(CO)₃H (**2b**), and (η^5 -C₅H₅)Cr(CO)₃H (**2c**). With a large excess of the deuterated olefin the first exchange goes to completion before subsequent exchanges begin, at a rate first order in olefin and in hydride. (Hydrogenation is insignificant except with styrene and CpCr(CO)₃H; in most cases, the radicals arising from the first H• transfer are too hindered to abstract another H•.) Statistical corrections give the rate constants k_{reinit} for H• transfer to the olefin from the hydride. With MMA, k_{reinit} decreases substantially as the steric bulk of the hydride increases; with styrene, the steric bulk of the hydride has little effect. At longer times, the reaction of MMA or styrene with **2a** gives the corresponding metalloradical **1a** as termination depletes the concentration of the methyl isobutryl radical **3** or the α -methylbenzyl radical **4**; computer simulation of [**1a**] as f(t) gives an estimate of k_{tr} , the rate constant for H• transfer from **3** or **4** back to Cr. These rate constants imply a ΔG (50 °C) of +11 kcal/mol for H• transfer from **2a** to MMA, and a ΔG (50 °C) of +10 kcal/mol for H• transfer from **2a** to styrene. The CH₃CN p*K*_a of **2a**, 11.7, implies a BDE for its Cr–H bond of 59.6 kcal/mol, and DFT calculations give 58.2 kcal/mol for the Cr–H bond in **2c**. In combination the kinetic ΔG values, the experimental BDE for **2a**, and the calculated ΔS values for H• transfer imply a C–H BDE of 45.6 kcal/mol for the methyl isobutryl radical **3** (close to the DFT-calculated 49.5 kcal/mol), and a C–H BDE of 47.9 kcal/mol for the α -methylbenzyl radical **4** (close to the DFT-calculated 49.9 kcal/mol). A solvent cage model suggests 46.1 kcal/mol as the C–H BDE for the chain-carrying radical in MMA polymerization.

Introduction

Metalloradicals have proven to be effective catalysts for chain transfer during free radical polymerizations.¹ Although the original (and most effective) chain transfer catalysts have been cobalt(II) complexes,² we have found that the hindered chromium metalloradical (η^5 -C₅Ph₅)Cr(CO)₃• (**1a**) is also an effective catalyst for chain transfer during the AIBN-initiated polymerization of methyl methacrylate.⁴ Recently Poli and co-workers have reported two Mo(III) complexes that are active chain-transfer catalysts during the polymerization of styrene.⁵

Chain-transfer catalysis is thought to involve removal of H• from the propagating radical chain, giving a vinyl-terminated polymer and a metal hydride (eq 1), followed by transfer of that H• to monomer to start a new chain (eq 2). Such catalysis reduces the molecular weight of the polymer.¹ In effect, the catalyst moves H• from the end of a growing chain to the beginning of a new one.



The instability of Co and Mo hydrides has made it difficult to observe eq 2 directly. We have, however, prepared (η^5 -C₅-Ph₅)Cr(CO)₃H (**2a**) and observed eq 2 directly by treating **2a** with methyl methacrylate (MMA) monomer.⁴ Heating a solution of (η^5 -C₅Ph₅)Cr(CO)₃H in MMA causes polymerization to

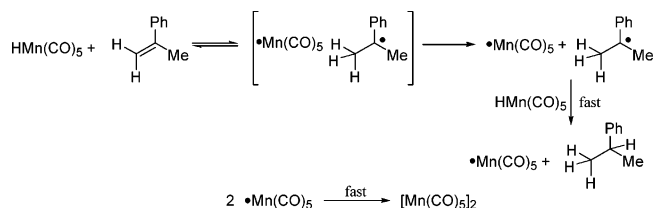
[†] Columbia University.

[‡] Colorado State University.

- (1) (a) Gridnev, A. A.; Ittel, S. D. *Chem. Rev.* **2001**, *101*, 3611–3659. (b) Gridnev, A. *J. Polymer Sci. Part A: Polym. Chem.* **2000**, *38*, 1753–1766.
- (2) (a) Enikolopyan, N. S.; Smirnov, B. R.; Ponomarev, G. V.; Bel'govskii, I. M. *J. Polym. Sci., Polym. Chem. Ed.* **1981**, *19*, 291. (b) Burczyk, A. F.; O'Driscoll, K. F.; Rempel, G. L. *J. Polym. Sci., Chem. Ed.* **1984**, *22*, 3255. (c) Gridnev, A. A. *Polym. Sci. U. S. S. R. (Engl. Transl.)* **1989**, *31*, 2369. For reviews see: (d) Karmilova, L. V.; Ponomarev, G. V.; Smirnov, B. R.; Belgovskii, I. M. *Russ. Chem. Rev. (Engl. Transl.)* **1984**, *53*, 132. (e) Moad, G.; Solomon, D. H. *The Chemistry of Free Radical Polymerization*; Pergamon: New York, 1995; Section 5.3.2.7.
- (3) Hoobler, R. J.; Hutton, M. A.; Dillard, M. M.; Castellani, M. P.; Rheingold, A. L.; Rieger, A. L.; Rieger, P. H.; Richards, T. C.; Geiger, W. E. *Organometallics* **1993**, *12*, 116–123.
- (4) Abramo, G. P.; Norton, J. R. *Macromolecules* **2000**, *33*, 2790–2792.

(5) Grognet, E. L.; Claverie, J.; Poli, R. *J. Am. Chem. Soc.* **2001**, *123*, 9513, and references therein.

Scheme 1



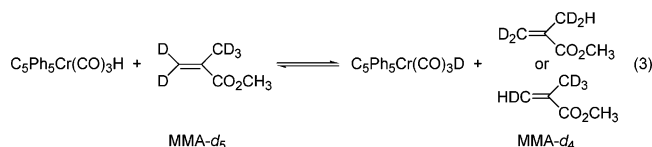
begin, along with the slow conversion of the hydride **2a** to the metalloradical **1a**.

There have been many previous reports of H• transfer from transition-metal hydrides to carbon–carbon double bonds, although the result has usually been hydrogenation. In 1975, Feder and Halpern proposed that the HCo(CO)₄-catalyzed hydrogenation of anthracene to 9,10-dihydroanthracene involved H• transfer.⁶ In 1977, Sweany and Halpern reported convincing evidence (CIDNP and an inverse isotope effect for HMn(CO)₅/DMn(CO)₅) for such a mechanism in the hydrogenation of α-methylstyrene by HMn(CO)₅ (Scheme 1).⁷ Other cases have been summarized in a review.⁸

To assess the ability of different metalloradicals to catalyze chain transfer, and to understand why (η⁵-C₅Ph₅)Cr(CO)₃H does not hydrogenate MMA when HMn(CO)₅ is known to hydrogenate α-methylstyrene, we have examined the kinetics and thermodynamics of the reactions of (η⁵-C₅R₅)Cr(CO)₃H (R = Ph, **2a**; R = Me, **2b**; R = H, **2c**) with MMA and styrene. This variation in the cyclopentadienyl substituent provides a large range of steric bulk in the hydride complexes.

Results and Discussion

H/D Exchange Between (η⁵-C₅R₅)Cr(CO)₃H (R = Ph, Me, H) (2a,b,c) and MMA-d₅. When a solution of the hydride **2a** in C₆D₆ was treated with a large excess (≥20 equiv) of MMA-d₅, ¹H NMR showed smooth decay of the hydride resonance and growth of the resonances of three isotopomers of MMA-d₄ (eq 3); the cis and trans isotopomers were formed in equal amounts. No methyl isobutyrate (which would be the product of hydrogenation) was observed



The first exchange proved cleanly separable from subsequent exchanges, i.e., an exponential fitted to the hydride resonance decayed to zero. The resulting rate constants (Table S1) and plot (Figure S1) confirm that exchange is first-order in MMA-d₅ (eq 4)

$$-\frac{d[\text{CrH}]}{dt} = k_1[\text{CrH}][\text{MMA-d}_5] \quad (4)$$

Extracting the rate constant k_{reinit} from an observed value of k_1 requires that we consider the fractional probability S that D• will return to the chromium metalloradical **1** after the initial transfer. S then relates k_1 to k_{reinit} as in eq 5

$$k_1 = S k_{\text{reinit}} \quad (5)$$

If we define k_{H} in Scheme 2 as the second-order rate constant for H• transfer to the metalloradical **1** from the deuterated methyl isobutryl radical **3-d₅**, and k_{D} as the second-order rate constant for D• transfer to **1** from **3-d₅**, then the selectivity factor S can be written as in eq 6. (We neglect any secondary isotope effects, and we defer consideration of cage effects.) By simplifying and dividing by k_{D} , S can be expressed in terms of $k_{\text{H}}/k_{\text{D}}$

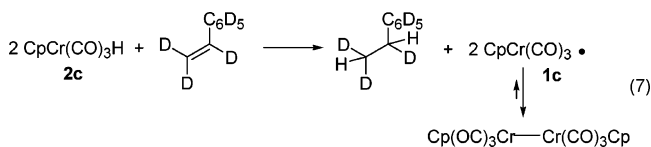
$$S = \frac{\frac{5}{6}k_{\text{D}}[\text{Cr}\cdot]}{\frac{5}{6}k_{\text{D}}[\text{Cr}\cdot] + \frac{1}{6}k_{\text{H}}[\text{Cr}\cdot]} = \frac{5}{5 + \frac{k_{\text{H}}}{k_{\text{D}}}} \approx \frac{5}{8} \quad (6)$$

Of course, k_{H} and k_{D} are related by a normal primary kinetic isotope effect. One estimate of its size can be obtained from the observed isotope effect (2.93) on the disproportionation rate constant for free radical polymerization of MMA at 60 °C.⁹ Another estimate (average value 3.5 between 40 and 80 °C) can be obtained by comparing the efficiency of a cobalt chain transfer catalyst for the polymerization of MMA with that for the polymerization of MMA-d₈.¹⁰ We have used the value of 3 shown in eq 6 to obtain the values of k_{reinit} in Table 1.

Similar results, also without hydrogenation, were observed when MMA-d₅ was treated with the hydride **2b** or **2c**. The resulting values of k_{reinit} are also in Table 1. Comparison of k_{reinit} for **2a**, **2b**, and **2c** at 323 K shows a substantial increase in the rate of H• transfer as we decrease the steric bulk of the hydride complex. (As will be seen, there is little variation in the Cr–H bond strengths.) The temperature dependence of the observed rate constants gives the activation parameters in Table 2.

Reaction of (η⁵-C₅R₅)Cr(CO)₃H (R = Ph, Me, H) (2a,b,c) with Styrene-d₈. In the case of styrene competition between hydrogenation and H/D exchange was observed. The bright blue color of (η⁵-C₅Ph₅)Cr(CO)₃• (**1a**) appeared within a few minutes of sealing an NMR tube with the C₅Ph₅ hydride **2a** and styrene-d₈, and traces of ethylbenzene could be seen in the ¹H NMR spectrum. With the C₅Me₅ hydride **2b** and styrene-d₈ more ethylbenzene was formed. Depending on the initial concentration we observed between 2 and 8% ethylbenzene in addition to the main product styrene-d₇.

When the C₅H₅ hydride **2c** was treated with styrene-d₈, the Cp peak broadened and gradually shifted downfield to δ7.5 before disappearing completely from the ¹H NMR spectrum (These results presumably arise from fast H• exchange between CpCr(CO)₃H and the product metalloradical CpCrCr(CO)₃• (**1c**), present in equilibrium with its dimer [CpCr(CO)₃]₂). Meanwhile, the hydride peak disappeared and ethylbenzene appeared (eq 7). A 2:1 ratio of **2c**:styrene resulted in complete hydrogenation to give the metalloradical **1c**, which is in equilibrium with its dimer (eq 7). Δ*G* for dissociation of the weak metal–metal bond in [CpCr(CO)₃]₂ is only 4.6 kcal/mol at 300 K, so there is only 10% monomer when [Cr] is 0.01 M¹¹

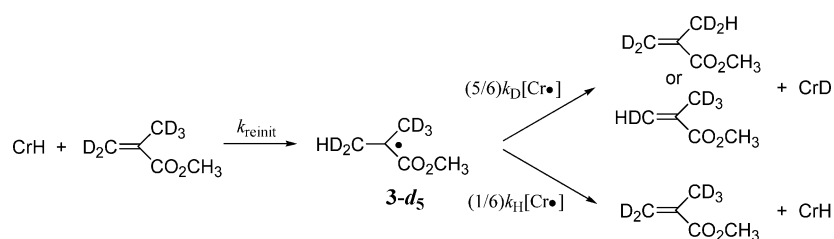


(6) Feder, H. M.; Halpern, J. J. *Am. Chem. Soc.* **1975**, *97*, 7186.

(7) Sweany, R. L.; Halpern, J. J. *Am. Chem. Soc.* **1977**, *99*, 8335.

(8) Eisenberg, D. C.; Norton, J. R. *Israel J. Chem.* **1991**, *31*, 55–66.

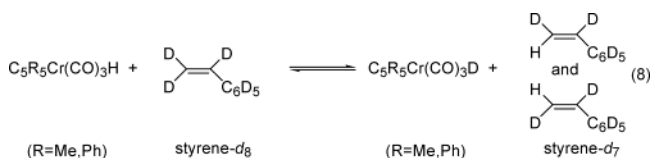
Scheme 2

**Table 1.** Values of k_{reinit} ^a from Isotopic Exchange between (η^5 -C₅R₅)Cr(CO)₃H and Excess MMA-*d*₅

<i>T</i> (K)	k_{reinit} (10 ⁻³ M ⁻¹ s ⁻¹)		
	R = Ph ^b	R = Me ^b	R = H ^c
333	3.00 (5)		
323	1.74 (8) ^d	2.61 (5)	
318	1.19 (2)	1.73 (1)	
313	0.73 (1)	0.94 (2)	
308	0.51 (1)	0.62 (1)	4.0 (2)
303		0.350 (6)	2.5 (1)
298			1.23 (4)
293			0.97 (3)
288			0.59 (3)

^a Obtained using eqs 4, 5, and 6. Figures in parentheses are standard deviation in least significant digit. ^b In C₆D₆. ^c In toluene-*d*₈. ^d From Figure S1.

Values of k_{reinit} for H• transfer to styrene can be extracted from the observed rate constants with styrene-*d*₈ by procedures similar to those in eqs 4–6. If we neglect hydrogenation and consider the overall reaction to be that in eq 8, then we need only consider the top part of Scheme 3; *S* for transfer to styrene will be given by eq 9 and the rate law for disappearance of the hydride resonance by eq 10. (Of course k_{H} and k_{D} now refer to the H• and D• transfer from the α -methylbenzyl radical 4-*d*₈).



$$S = \frac{\frac{2}{3}k_{\text{D}}[\text{Cr}\bullet]}{\frac{1}{3}k_{\text{H}}[\text{Cr}\bullet] + \frac{2}{3}k_{\text{D}}[\text{Cr}\bullet]} = \frac{2}{\frac{k_{\text{H}}}{k_{\text{D}}} + 2} \approx \frac{2}{5} \quad (9)$$

$$k_{\text{obs}} = k_{\text{reinit}}[\text{styrene-}d_8]S \quad (10)$$

$$-\frac{d[2\text{c}]}{dt} = 2k_{\text{reinit}}[2\text{c}][\text{styrene-}d_8] \quad (11)$$

When, as with the C₅H₅ hydride **2c**, hydrogenation is complete we need only consider the bottom part of Scheme 3, and can write the rate law in eq 11 and thereby calculate the values of k_{reinit} in Table 3 below.

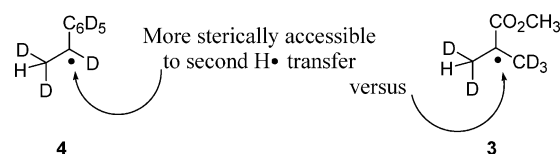
Table 2. Activation Parameters and k_{reinit} at 323 K for Isotopic Exchange between (η^5 -C₅R₅)Cr(CO)₃H and Excess MMA-*d*₅

R	k_{reinit} (323K), 10 ⁻³ M ⁻¹ s ⁻¹	ΔH^\ddagger , kcal/mol	ΔS^\ddagger , eu
Ph	1.74 (8) ^a	14.1 (8)	-28 (3)
Me	2.61 (5) ^a	19.0 (6)	-12 (2)
H	14 (3) ^b	16 (1)	-17 (5)

^a Uncertainties from 323 K points in Table 1. ^b Extrapolated from activation parameters. Uncertainties take into account covariance between ΔH^\ddagger and ΔS^\ddagger .

With the C₅Ph₅ hydride **2a** it is clearly appropriate to calculate k_{reinit} from eq 10. With the C₅Me₅ hydride **2b** we have still used eq 10; the error introduced thereby should be $\leq 5\%$. The results are collected in Table 3.

For styrene k_{reinit} from the hydride **2a** is about an order of magnitude faster than for MMA. However, in contrast to our observations with MMA, there is little variation in k_{reinit} with the steric bulk of the hydride complex—presumably because the double bond in styrene has fewer substituents. Completion of hydrogenation by transfer of a second H• to the methyl isobutyl radical **3** in Scheme 2 or the α -methylbenzyl radical **4** in Scheme 3—is not appreciable except in the least crowded case, the C₅H₅ hydride **2c** and styrene. A considerable difference between **3** and **4** is apparent



Formation of (η^5 -C₅Ph₅)Cr(CO)₃• (1a) from (η^5 -C₅Ph₅)-Cr(CO)₃H (2a) and MMA. Kinetic Modeling. As we previously reported,⁴ the hydride **2a** can initiate polymerization in neat MMA. When heated to 100 °C under an inert atmosphere, a 1.15 × 10⁻⁴ M solution of **2a** in MMA turned from light green to blue, the color characteristic of the metalloradical **1a**; IR confirmed that **1a** had been formed. Use of the extinction coefficient of **1a** at 611 nm, determined in toluene as 720(80) M⁻¹ cm⁻¹, suggested that the conversion of **2a** to **1a** was over 90%. Removal of excess monomer after 1 h afforded PMMA with a number average molecular weight of approximately 6500, close to the number average molecular weight from an AIBN-initiated polymerization in the presence of a similar concentration of the metalloradical **1a**.⁴

Similar conversions were obtained in a series of experiments at lower temperatures, from 50 to 75 °C. Over a reaction time of 8–12 h, 10–25% of the monomer was typically converted to polymer.

At 65 °C with the hydride **2a** in neat MMA the appearance of the metalloradical **1a** was monitored by UV–vis spectroscopy

- (9) Ayrey, G.; Wong, D. J. D. *Polymer* **1975**, *16*, 623.
 (10) Gridnev, A. A.; Ittel, S. D.; Wayland, B. B.; Fryd, M. *Organometallics* **1996**, *15*, 5116.
 (11) (a) Adams, R. D.; Collins, D. E.; Cotton, F. A. *J. Am. Chem. Soc.* **1974**, *96*, 749. (b) Landrum, J. T.; Hoff, C. D. *J. Organomet. Chem.* **1985**, *282*, 215. (c) Madach, T.; Vahrenkamp, H. Z. *Naturforsch. B.: Anorg. Chem., Org. Chem.* **1978**, *33B*, 1301. (d) McLain, S. J. *J. Am. Chem. Soc.* **1988**, *110*, 643. (e) Woska, D. C.; Ni, Y.; Wayland, B. B. *Inorg. Chem.* **1999**, *38*, 4135.

Scheme 3

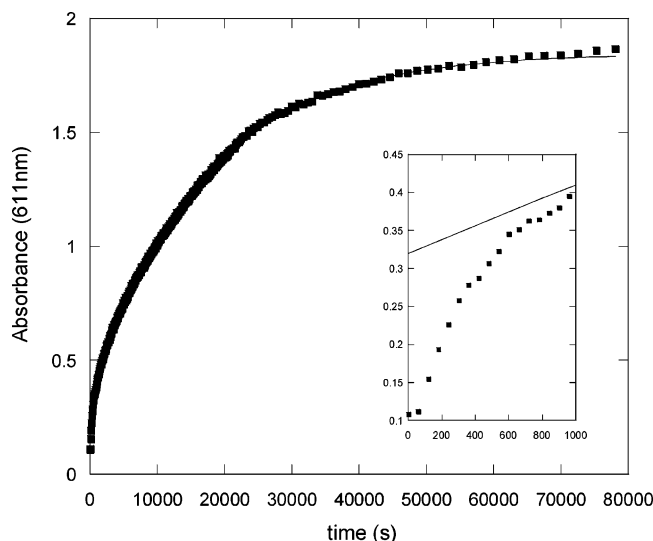
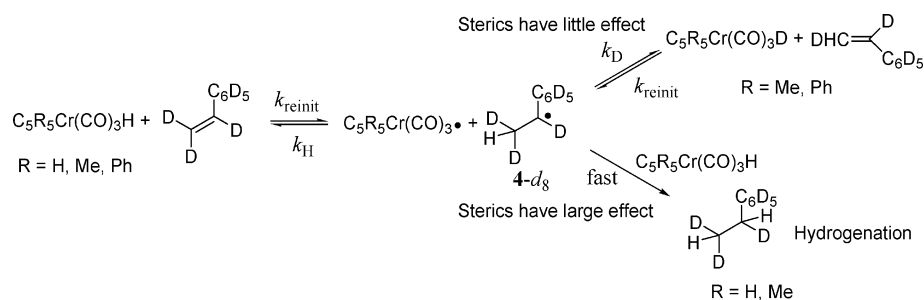


Figure 1. Absorbance of **1a** at 611 nm (■) as a function of time when a solution of **2a** ($[\mathbf{2a}]_0 = 3.6 \times 10^{-3}$ M) in neat MMA is heated at 65 °C. (The solid line is the exponential curve fit.) The initial 1000 s are shown in the inset.

Table 3. Values of k_{reinit} for $(\eta^5\text{-C}_5\text{R}_5)\text{Cr}(\text{CO})_3\text{H}$ ($\text{R} = \text{H, Me, Ph}$) and Excess Styrene- d_8 in C_6D_6

T (K)	k_{reinit} ($10^{-3} \text{ M}^{-1} \text{ s}^{-1}$)		
	$\text{R} = \text{Ph}^b$	$\text{R} = \text{Me}^b$	$\text{R} = \text{H}^c$
323	18.4 (9) ^a	5.4 (3)	15.8 (6)
318			10.5 (3)
313	11.8 (7) ^a	4.6 (2)	6.3 (5)
308			5.6 (3)
303	7.2 (2)	3.6 (2)	3.7 (3)

^a Average of two measurements. ^b Obtained using eq 9, 10. ^c Obtained using eq 11.

(Figure 1). There was a significant deviation from exponential behavior (see inset) at short reaction times.¹²

Using a solution of MMA in toluene instead of neat MMA decreased the extent to which chain growth (rate constant $k_{\text{p}}[\text{MMA}]$) competed with $\text{H}\cdot$ return (rate constant $k_{\text{tr}}[\text{Cr}\cdot]$) for the methyl isobutyryl radical **3**. We were thus able to watch the growth of the metalloradical **1a** (20% to 30% conversion) without significant changes in $[\text{MMA}]$, and to determine the

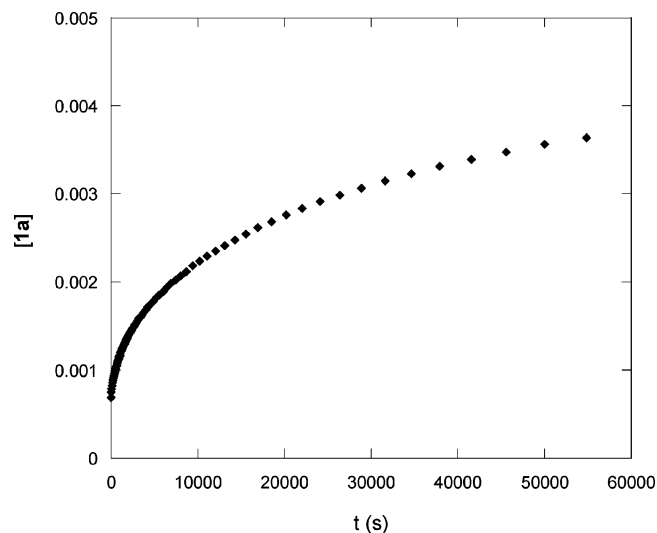
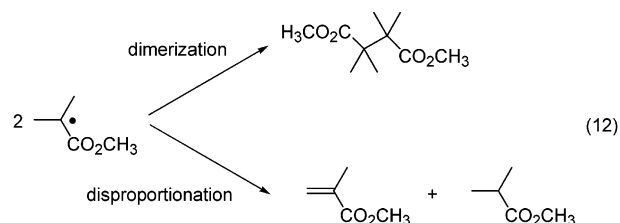


Figure 2. UV kinetic trace for the reaction of **2a** (0.0121 M) with MMA (0.268 M) in toluene at 50 °C. (Concentration of **1a** from visible absorbance at 611 nm ♦).

kinetics of $\text{H}\cdot$ transfer in both directions. A typical plot of $[\mathbf{1a}]$ as a function of time is shown in Figure 2.

The $\text{H}\cdot$ transfer is thermodynamically *uphill* (see below), and the hydride **2a** converts to the metalloradical **1a** only because the methyl isobutyryl radicals **3** are consumed by dimerization and disproportionation reactions (eq 12). The rate constant at 50 °C for both processes combined is $3.3 \times 10^7 \text{ M}^{-1} \text{ s}^{-1}$ for polymers with P_n (number average degree of polymerization) = $10^{4.13}$ but it increases as the chain length decreases—by about a factor of 5 for chain lengths as short as the ones in this experiment,¹⁴ making k_{term} equal to $1.65 \times 10^8 \text{ M}^{-1} \text{ s}^{-1}$. The concentration of MMA is sufficiently high, and the conversion so low, that to a first approximation we can neglect the reformation of MMA by eq 12. If we use k_{reinit} as $0.0017 \text{ M}^{-1} \text{ s}^{-1}$ from Table 1, and simulate¹⁵ the growth of the metalloradical **1a** as illustrated in Scheme 4, we can determine k_{tr} by iteration

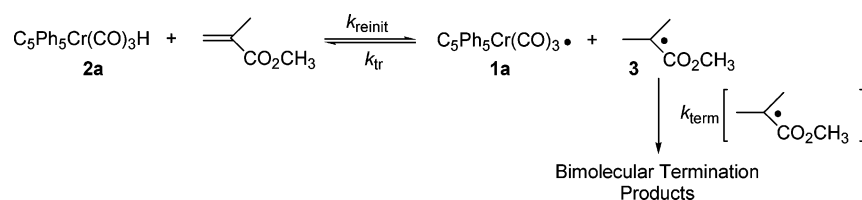


The resulting values of k_{tr} , from experiments over a wide range of initial MMA concentrations, are shown in Table 4. (A

(12) Kinetic modelling with $[\text{MMA}] = 9.3 \text{ M}$ and the rate constants given in this section produces (Figure S3) an initial sharp rise in $[\mathbf{1a}]$ like that observed in Figure 1, although the agreement is not perfect (in neat MMA polymerization changes the viscosity and significantly decreases $[\text{MMA}]$, making modelling difficult). High $[\text{MMA}]$ pushes the equilibrium far enough to the right that the rapid operation of k_{reinit} and k_{tr} generates significant **1a** before k_{term} begins to consume **3**; as we would expect, no such initial rise in $[\mathbf{1a}]$ is seen in the subsequent experiments at lower $[\text{MMA}]$ in toluene.

(13) Extrapolated to 50 °C from equation given by Mahabadi, H. K.; O'Driscoll, K. F. *J. Macromol. Sci. A: Chem.* **1977**, *11*, 967–976.

Scheme 4

**Table 4.** Values of k_{tr}^a from MacKinetics¹⁵ Iteration of the Reaction of (η^5 -C₅Ph₅)Cr(CO)₃H (**2a**) with MMA in Toluene at 50 °C

[2a] _{init} (10 ⁻³ M)	[MMA] _{init} (M)	k_{tr} (10 ³ M ⁻¹ s ⁻¹)
11.4	0.268	114
9.30	0.318	88.7
9.00	0.0791	38.2
6.52	0.281	128
8.35	0.212	84.3
9.15	0.186	91.0
8.56	0.221	94.7

^a $k_{\text{reinit}} = 0.0017 \text{ M}^{-1}\text{s}^{-1}$, $k_{\text{term}} = 1.65 \times 10^8 \text{ M}^{-1}\text{s}^{-1}$, ϵ of **1a** = 720 M⁻¹cm⁻¹.

sample MacKinetics fit plot (Fig S4) is available in the Supporting Information.) They have an average of 91 000 M⁻¹s⁻¹. The major source of uncertainty is the k_{term} estimate; however, changing k_{term} by a factor of 2 only changes k_{tr} by 30%.

Kinetic Modeling of the Formation (η^5 -C₅Ph₅)Cr(CO)₃• (1a**) from (η^5 -C₅Ph₅)Cr(CO)₃H (**2a**) and Styrene.** The metallocoradical **1a** was also formed when a toluene solution of styrene and the hydride **2a** was heated at 50 °C. Monitoring the reaction by UV–vis spectroscopy, and taking $\epsilon(\mathbf{1a})$ at 611 nm in toluene as 720 M⁻¹cm⁻¹, k_{reinit} as 0.018 M⁻¹s⁻¹ from Table 3, and k_{term} (Scheme 5) as $3.2 \times 10^7 \text{ M}^{-1}\text{s}^{-1}$,¹⁶ we can simulate the growth of **1a** as shown in Scheme 5. For the data set presented a k_{tr} of 84 000 M⁻¹s⁻¹ gives the best fit. As was the case with MMA, changing k_{term} by a factor of 2 only changes k_{tr} by 30%.

Thermodynamics of the H• Transfer Equilibrium: Bond Strengths. The position of a reversible H• transfer equilibrium like Schemes 4 or 5 depends on the strength of the Cr–H and C–H bonds that are broken and made. To a first approximation, assuming $\Delta S \approx 0$, we can express ΔG for such an equilibrium by eq 13, where BDE(C–H) is the bond dissociation energy of the C–H bond in the methyl isobutyl radical **3** or the α -methylbenzyl radical **4**. Our experiments thus offer a way of obtaining the BDE(C–H) of unstable radicals **3** and **4**

$$\Delta G = \Delta H = \text{BDE}(\text{Cr–H}) - \text{BDE}(\text{C–H}) \quad (13)$$

Computation of Cr–H and C–H Bond Strengths. Computational methods, in particular those using density functional theory (DFT),¹⁷ have become popular in recent years for computing BDEs of a variety of molecules including transition

metal complexes¹⁸ and have provided access to absolute energy values without having to neglect the entropy changes as above. Because absolute energies obtained in quantum chemical calculations are quite sensitive to the level of theory employed, comparisons of reported BDEs from different studies are problematic. Thus, we have computed both the Cr–H and C–H bond strengths with the goal of obtaining values for the bond strengths at the same level of theory to compare with those derived from experimental methods. Because of computational demands, however, the Cr–H bond strength has been computed only for (η^5 -C₅H₅)Cr(CO)₃H. Bond dissociation processes require corrections for vibrational zero point energy (ZPE) changes to the enthalpy, which are accessible by computing the vibrational frequencies of all species involved. These computed frequencies also provide reasonable estimates for vibrational entropies and, thus, allow the explicit evaluation of free energies of bond dissociation within the usual framework of the standard approximations of statistical thermodynamics.

For our Cr–H and C–H bonds the computed values are summarized in Table 5 and the individual energy corrections are listed in the Supporting Information. Calculated contributions of the entropy to the bond dissociation indicate that the ΔS values for the H• transfer reactions depicted in Schemes 4 and 5 are +2.36 and +1.65 kcal/mol at 298 K, respectively. The computed bond dissociation energy terms indicate that changes of the intrinsic entropy components, that is the vibrational, rotational, and translational entropies of the molecule, are of the same order of magnitude as the solvation free energy changes upon bond dissociation. As can be expected, the entropies favor the dissociated (H•) side of the reaction, while solvation favors the reactant (M–H or C–H) side. Note that the solvation free energy of H• is positive (estimated to be +5.12 kcal/mol in water¹⁹).

Determination of Cr–H Bond Strength in (η^5 -C₅Ph₅)Cr(CO)₃H (2a**).** Experimentally, it is straightforward to determine the strength of the Cr–H bond in **2a** from a thermodynamic cycle involving the pK_a of the hydride and the redox potential of the anion (the conjugate base of **2a**). Breslow and co-workers initially used such cycles to estimate the pK_a values of some weak carbon acids,²⁰ Bordwell and co-workers have used such cycles to estimate many C–H bond strengths in DMSO,²¹ and Tilset and Parker,²² as well as Protasiewicz and Theopold,²³ have estimated many M–H solution bond dissociation energies in this way.

(18) Ziegler, T. *Chem. Rev.* **1991**, 91, 651–667.

(19) Brunner, E. J. *Chem. Eng. Data* **1985**, 30, 269.

(20) (a) Breslow, R.; Balasubramanian, K. *J. Am. Chem. Soc.* **1969**, 91, 5182. (b) Breslow, R.; Chu, W. *J. Am. Chem. Soc.* **1973**, 95, 411. (c) Jaun, B.; Schwarz, J.; Breslow, R. *J. Am. Chem. Soc.* **1980**, 102, 5741–5748.

(21) Bordwell, F. G.; Cheng, J. P.; Harrelson, J. A., Jr. *J. Am. Chem. Soc.* **1988**, 110, 1229.

(22) (a) Tilset, M.; Parker, V. D. *J. Am. Chem. Soc.* **1989**, 111, 6711, as modified by (b) Tilset, M.; Parker, V. D. *J. Am. Chem. Soc.* **1990**, 112, 2843. Potential sources of error in the determination of M–H bond strengths by this method have been reviewed in ref 8 above.

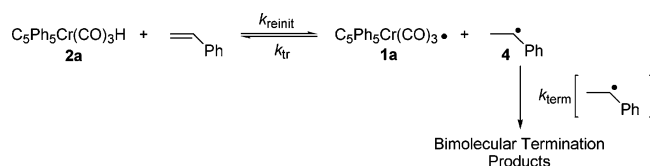
(23) Protasiewicz, J. D.; Theopold, K. H. *J. Am. Chem. Soc.* **1993**, 115, 5559.

- (14) By extrapolation from the MMA/toluene data in Figure 2 and Table 3 in Suddaby, K. G.; Maloney, D. R.; Haddleton, D. M. *Macromolecules* **1997**, 30, 702–713. From polymerizations with the same [Cr•] we calculate P_n as 2 (at such high concentrations of chain transfer catalyst P_n is very small).
- (15) MacKinetics, written by and obtained from Leipold, W. S., III.; Weiher, J. F.; McKinney, R. J. E. I. du Pont de Nemours, Inc., 1992–1995.
- (16) Matheson, M. S.; Auer, E. E.; Bevilacqua, E. B.; Hart, E. J. *J. Am. Chem. Soc.* **1951**, 73, 1700.
- (17) Parr, R. G.; Yang, W. *Density Functional Theory of Atoms and Molecules*; Oxford University Press: New York, 1989.

Table 5. DFT-calculated Gas Phase Bond Dissociation Enthalpy (ΔH), Entropy (ΔS), and Free Energy (ΔG), Solution Phase Bond Dissociation Enthalpy ($\Delta H(\text{sol})$) and Solution Phase Bond Dissociation Free Energy ($\Delta G(\text{sol})$)

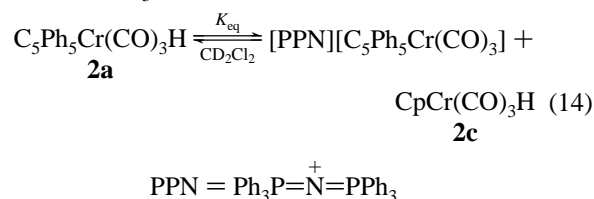
$X\bullet$	$\Delta H(\text{gas})$ (kcal/mol)	$\Delta H(\text{sol})^a$ (kcal/mol)	$-\Delta S(\text{gas})$ (kcal/mol)	$\Delta G(\text{gas})$ (kcal/mol)	$\Delta G(\text{sol})^a$ (kcal/mol)
$(\eta^5\text{-C}_5\text{H}_5)\text{Cr}(\text{CO})_3$	54.42	57.55/58.18	−8.56	45.86	48.99/49.62
methylisobutryl	45.83	49.48/49.79	−6.20	39.64	43.28/43.59
α -methylbenzyl	46.77	49.91/49.67	−6.91	39.86	43.00/42.76

All calculations are done for the reaction $\text{XH} \rightarrow \text{X}\bullet + \text{H}\bullet$, where X denotes different fragments. See Computational Details for definitions of the energy terms. ^a The solution phase values are given both for toluene and acetonitrile; toluene values are listed first, followed by those for acetonitrile.

Scheme 5

Determining the $\text{p}K_a$ of **2a** proved unusually difficult because **2a** is insoluble in CH_3CN (the solvent we have preferred in our previous measurements²⁴ of the thermodynamic acidity of transition-metal hydrides). We therefore monitored the equilibrium K_{eq} for deprotonation of **2a** by $[\text{PPN}][\text{CpCr}(\text{CO})_3]$ (the conjugate base of **2c**) (eq 14) over a range of temperatures by ^1H NMR in CD_2Cl_2 . (Measurement of K_{eq} by IR in CH_2Cl_2 proved impractical because of overlap of the peaks of both hydrides and their anions.) From -50 to 0°C , the cyclopentadienyl signals belonging to $\text{CpCr}(\text{CO})_3\text{H}$ (**2c**) and $[\text{PPN}][\text{CpCr}(\text{CO})_3]$ could be integrated separately and K_{eq} determined from their ratio and the initial concentrations of **2a** and $[\text{PPN}][\text{CpCr}(\text{CO})_3]$

$[\text{PPN}][\text{CpCr}(\text{CO})_3] +$

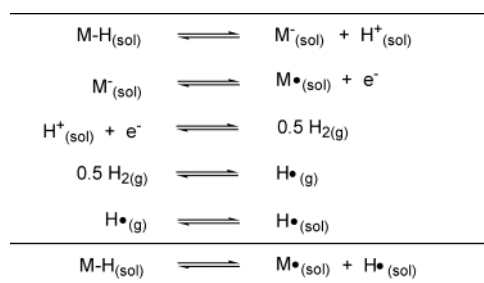


The value of K_{eq} (80) measured at 250 K was corrected to 298 K by assuming ΔG to be approximately constant and using $\Delta G = -RT \ln K_{\text{eq}}$. If we assume that for such large bases K_{eq} will be similar in CH_2Cl_2 and CH_3CN ,^{23,25} and take the $\text{p}K_a$ of **2c** in CH_3CN as 13.3,²⁴ then we can estimate the $\text{p}K_a$ of **2a** in CH_3CN as 11.7(3).

The thermodynamic cycle in Scheme 6 yields eq 15 if we add the reactions and substitution the appropriate physical constants²²

$$\text{BDE}(\text{M}-\text{H}) = 1.37 \text{ p}K_a(\text{M}-\text{H}) + 23.06 \text{ E}^\circ(\text{M}\bullet/\text{M}^-) + 58.4 \text{ kcal/mol} \quad (15)$$

The known redox potential of $\text{C}_5\text{Ph}_5\text{Cr}(\text{CO})_3\bullet/\text{C}_5\text{Ph}_5\text{Cr}(\text{CO})_3^-$

Scheme 6**Table 6.** BDE of Different Cr Hydrides

Cr hydride	BDE, kcal/mol
$\text{H}-\text{Cr}(\text{CO})_3(\text{C}_5\text{Ph}_5)^a$	59.6 (3)
$\text{H}-\text{Cr}(\text{CO})_3(\text{C}_5\text{Me}_5)^{28}$	62.3
$\text{H}-\text{Cr}(\text{CO})_3(\text{C}_5\text{H}_5)^b$	61.5
$\text{H}-\text{Cr}(\text{CO})_2(\text{PPh}_3)(\text{C}_5\text{H}_5)^b$	59.8
$\text{H}-\text{Cr}(\text{CO})_2(\text{PEt}_3)(\text{C}_5\text{H}_5)^b$	59.9
$\text{H}-\text{Cr}(\text{CO})_2(\text{POMe})_3(\text{C}_5\text{H}_5)^b$	62.7

^a This work, in CH_3CN . ^b The rest of the BDE values are from ref 27 and are in toluene.

in CH_3CN ,^{3,26} and our $\text{p}K_a$ estimate in the same solvent yield a **Cr–H bond dissociation energy** of 59.6(3) kcal/mol in CH_3CN . In good agreement with this value, our DFT calculation predicts a BDE of 58.2 kcal/mol in CH_3CN (Table 5). Furthermore, our experimental value for **2a** fits well with calorimetric determinations on related chromium hydrides (Table 6).²⁷ In the Hoff study, the monomer–dimer equilibrium of $[(\eta^5\text{-C}_5\text{Me}_5)\text{Cr}(\text{CO})_3]_2$ was used to measure the Cr–Cr bond enthalpy,²⁸ and the enthalpy of reaction of the $(\eta^5\text{-C}_5\text{Me}_5)\text{Cr}(\text{CO})_3\bullet$ radical with H_2 was measured calorimetrically, so the value of 62.3 for the Cr–H BDE of $\text{C}_5\text{Me}_5\text{Cr}(\text{CO})_3\text{H}$ in toluene should be quite accurate. In the same study, the Cr–H BDE of $\text{CpCr}(\text{CO})_3\text{H}$ was also determined to be 61.5 kcal/mol in toluene, which compares reasonably well to our DFT value of 57.6 kcal/mol for toluene (Table 5). The agreement between the calorimetric numbers, our BDE value derived from the K_{eq} measurement and DFT-computed numbers gives reassurance that the assumptions used in the proton-transfer treatment are reasonable.

Strength of the C–H Bond in the Methyl Isobutryl Radical 3. The literature yields conflicting evidence about the strength of the C–H bond in **3**. Of course we can obtain that bond strength if we know the heats of formation of both sides of eq 16. The gas-phase enthalpy of formation of methyl

(24) The work has been summarized in a review: Kristjánssdóttir, S. S.; Norton, J. R. "Acidity of Hydrido Transition Metal Complexes in Solution". In *Transition Metal Hydrides*; Dedieu, A., Ed.; VCH: New York, 1991; Chapter 9.

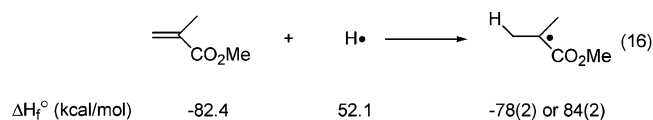
(25) Proton-transfer equilibria of η^2 -dihydrogen complexes measured in CD_2Cl_2 have been used to estimate aqueous $\text{p}K_a$ values in the same fashion: Jia, G.; Morris, R. H. *Inorg. Chem.* **1990**, 29, 582–584.

(26) To convert the redox potential of **1** vs (Fc/Fc^+) in CH_3CN to a redox potential vs (H^+/H_2) in CH_3CN a value of 0.049 V is added. Kiolthoff, I. M.; Chantooni, M. K., Jr. *J. Phys. Chem.* **1972**, 76, 2024–2034.

(27) Kiss, G.; Zhang, K.; Mukerjee, S. L.; Hoff, C. D. *J. Am. Chem. Soc.* **1990**, 112, 5657–5658.

(28) Watkins, W. C.; Jaeger, T.; Kidd, C. E.; Fortier, S.; Baird, M. C.; Kiss, G.; Roper, G. C.; Hoff, C. D. *J. Am. Chem. Soc.* **1992**, 114, 907–914.

methacrylate is -82.4 kcal/mol,²⁹ but the gas-phase enthalpy of formation of a methyl isobutyryl radical **3** is less accurately known. Engel and co-workers have calculated $-78(2)$ kcal/mol³⁰ by using -111 kcal/mol³¹ as the enthalpy of formation of methyl isobutyrate and estimating³² the C–H BDE for the tertiary carbon of methyl isobutyrate as 85 kcal/mol. By using the same C–H BDE of 85 kcal/mol, but using the enthalpy of formation of methyl isobutyrate (-117.3 kcal/mol) measured calorimetrically by Kharasch,³³ one can calculate a value of $-84(2)$ kcal/mol for the enthalpy of formation of the methyl isobutyryl radical. Combining either of these two values for **3** with 52.1 kcal/mol for H• implies that the gas-phase C–H BDE in the methyl isobutyryl radical **3** is 48 or 54 kcal/mol. Our DFT calculations give a gas-phase BDE of 45.8 kcal/mol (Table 5), which is in better agreement with the former estimate



Comparing our Cr–H BDE (59.6 kcal/mol in CH₃CN) with any of these C–H results for methyl isobutyryl radical **3** makes it clear that the equilibrium in eq 17 is uphill, and that treatment of the hydride **2a** with MMA converts it to the metalloradical **1a** only because of the operation of k_{term} (Scheme 4). Comparison of the Cr–H and C–H DFT calculations in Table 5 suggests a gas phase ΔH for reaction 17 of 8.6 kcal/mol. Addition of ΔS and solvation energies from the continuum solvation model gives an overall theoretical ΔG of 6.3 kcal/mol for the equilibrium in eq 17 in toluene (Table S10)

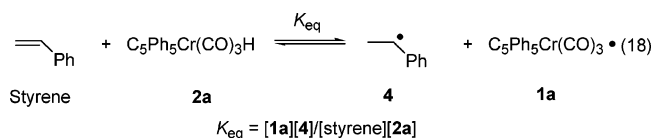


If we assume that $K_{\text{eq}} = k_{\text{reinit}}/k_{\text{tr}}$, our rate constants at 50 °C in toluene imply a value of 11.4 kcal/mol for ΔG (eq 17) at that temperature. Converting this number to a BDE requires that we separate the enthalpic and entropic contributions. In eq 13 we assumed $\Delta S \approx 0$, making ΔG and ΔH the same. A second possibility is to define an “experiment/theory hybrid” by using the DFT-computed gas phase ΔS of 7.93 eu (from Table S10) for the reaction shown in eq 17. If we begin with our experimental ΔG in toluene, estimate ΔS in that solvent from the gas-phase value, and assume that our Cr–H BDE in CH₃CN (59.6 kcal/mol) is approximately correct in toluene, then we obtain a C–H bond strength for methyl isobutyryl radical **3** of 45.6 kcal/mol in toluene, which is in reasonable agreement with our 49.5 kcal/mol in that solvent from DFT computations (Table 5).

Strength of the C–H Bond in the α -Methylbenzyl Radical

4. We can similarly infer the strength of the C–H bond in the α -methylbenzyl radical **4**. Reported C–H BDE's are as high as 54.3 kcal/mol and as low as 46.9 kcal/mol. The former number comes from the gas phase heats of formation (kcal/mol) of styrene (35.2),³⁴ H• (52.1), and the α -methylbenzyl radical (33).³⁵ This value (54 kcal/mol) is also supported by the equilibrium constant for the reversible decomposition of a Co(III)(α -phenethyl) complex to liberate styrene and half an equivalent of H₂.³⁶ The lower experimental estimate for the C–H BDE of α -methylbenzyl radical **4**, 46.9 kcal/mol, comes from a ΔH_f for this radical derived from very-low-pressure pyrolysis, 39.6 kcal/mol.³⁷ A similar value (41.3 kcal/mol) comes from proton affinity experiments by a thermodynamic cycle.³⁸ In good agreement with previous quantum chemical studies on MP4/CBS-4 level of theory³⁹ that reported a bond dissociation energy of 45.5 kcal/mol for α -methylbenzyl radical **4**, our DFT calculations suggest a gas-phase BDE of 46.8 kcal/mol, and lend support to the lower values in the set of estimates.

Comparing our Cr–H BDE (59.6 kcal/mol in CH₃CN) with the C–H BDE values from our DFT calculations and with literature bond strength estimates suggests that H• transfer from (η^5 -C₅Ph₅)Cr(CO)₃H to styrene (eq 18) is between 5 and 14 kcal/mol uphill. This range is slightly lower than an estimate, 16.1(4) kcal/mole, that has been published⁴⁰ for a similar H• transfer, between **2c** and α -cyclopropyl styrene



If we again assume that $K_{\text{eq}} = k_{\text{reinit}}/k_{\text{tr}}$, our rate constants at 50 °C in toluene imply a value of 9.87 kcal/mol for ΔG (eq 18) at that temperature. Now our “experiment/theory hybrid”, using ΔS from our gas-phase DFT computations (5.54 eu) and our Cr–H BDE from CH₃CN (59.6 kcal/mol), gives a C–H bond strength for **4** of 47.9 kcal/mol in toluene, which is in good agreement with our 49.9 kcal/mol in that solvent from DFT calculations.

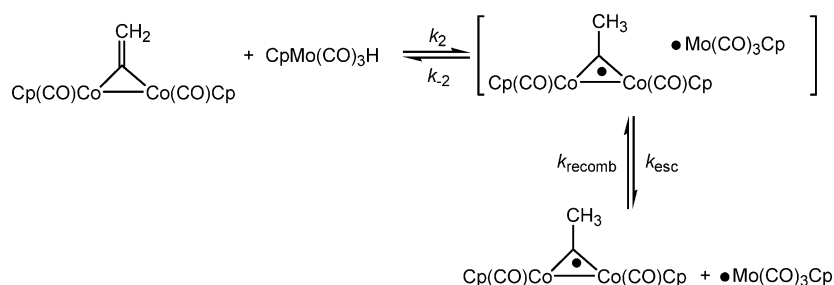
The β C–H bonds in the methyl isobutyryl radical **3** and the α -methylbenzyl radical **4** are both much weaker than ordinary C–H bonds. They are, however, stronger than the β C–H bond in the ethyl radical (35.7 kcal/mol).⁴¹

Cage Effects and their Influence on the Kinetic Determination of Bond Strengths. In Schemes 4 and 5 and eqs 17 and 18 we have assumed that the rate constant k_{reinit} corresponds to a single step. There are, however, many reasons to assume that such H• transfers occur within a solvent cage. The observation of CIDNP in Scheme 1 and related reactions^{7,8} implies competition between H• return and cage escape after H• transfer. Exchange between the hydride ligand and the substrate (ac-

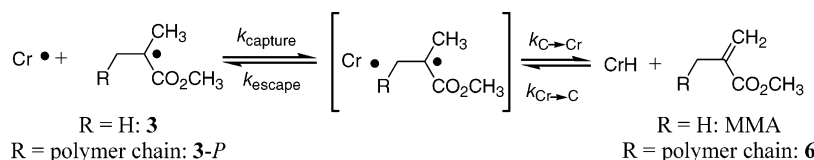
- (29) Viclu, R.; Perisanu, S. *Rev. Roumaine Chimie* **1980**, 25, 619–624.
 (30) Engel, P. S.; Chen, Y.; Wang, C. *J. Org. Chem.* **1991**, 56, 3073–3079.
 (31) Group addition thermochemical calculation using data from and methods of Pedley, J. B.; Naylor, R. D.; Kirby, S. P. *Thermochemical Data of Organic Compounds*; Chapman and Hall: London, 1986. This type of estimate should approximate the gas-phase enthalpy of formation.
 (32) The C–H BDEs were estimated using three different approaches: thermolysis of azoalkanes, thermolysis of dimethyl tetramethylsuccinate, and ESR determination of carboalkoxyalkyl radical rotational barriers.
 (33) Kharasch, M. S. *J. Res. Natl. Bur. Stand.* **1929**, 2, 359–430. It is unclear from the tables of thermodynamic data if the Kharasch measurement is a gas-phase enthalpy. If it is a condensed-phase measurement, then the heat of vaporization of methyl isobutyrate must be added to the measured value of -117.3 kcal/mol, which would essentially make the Engel and Kharasch numbers equal.

- (34) Prosen, E. J.; Rossini, F. P. *J. Res. Natl. Bur. Stand.* **1945**, 34, 59.
 (35) Kerr, J. A. *Chem. Rev.* **1966**, 66, 465.
 (36) Ng, F. T. T.; Rempel, G. L.; Mancuso, C.; Halpern, J. *Organometallics* **1990**, 9, 2762.
 (37) Robaugh, D. A.; Stein, S. E. *Int. J. Chem. Kinetics* **1981**, 13, 445–462.
 (38) Meot-Ner, M. *J. Am. Chem. Soc.* **1982**, 104, 5–10.
 (39) Zhang, X. M. *J. Org. Chem.* **1998**, 63, 1872–1877.
 (40) Bullock, R. M.; Samsel, E. G. *J. Am. Chem. Soc.* **1990**, 112, 6886–6898.
 (41) Blanksby, S. J.; Ellison, G. B. *Acc. Chem. Res.* **2003**, 36, 255–263.

Scheme 7



Scheme 8



complicated by the k_2 and k_{-2} steps) is considerably faster than the overall reaction in the system in Scheme 7.⁴²

Such cage effects may explain the difference between the k_{tr} value we obtained above ($9.1 \times 10^4 \text{ M}^{-1}\text{s}^{-1}$ by kinetic modeling) for methyl isobutryl radical **3** and the one we have obtained ($1.6 \times 10^6 \text{ M}^{-1}\text{s}^{-1}$ from molecular weight measurements as a function of [I]) for the polymer-containing radical **3-P**.⁴³ Cage effects may also explain why our $k_{tr}(\text{polymer})$ value decreases with temperature. The forward step (and by microscopic reversibility the reverse step) in reactions 17 and 18 may occur in *more than one step*, and may involve an associative pre-equilibrium;⁴⁴ if $\text{H}\bullet$ transfer occurs only after the formation of a solvent cage, then we have the sequence of events in Scheme 8. The first step k_{capture} is merely the microscopic reverse of cage escape, driven by the interaction between the metal-loradical $\text{Cr}\bullet$ and the chain-carrying radical **3-P**.^{45–47}

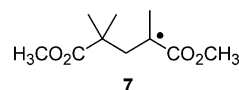
The observed rate constant k_{tr} will then be given by eq 19. The cage-forming equilibrium $k_{\text{capture}}/k_{\text{escape}}$ will lie further to the left with increasing temperature, making $k_{tr}(\text{polymer})$ decrease with increasing temperature as observed

$$k_{tr} = \frac{k_{\text{capture}}k_{\text{C-H-Cr}}}{k_{\text{escape}} + k_{\text{C-H-Cr}}} \approx \frac{k_{\text{capture}}k_{\text{C-H-Cr}}}{k_{\text{escape}}} \quad (19)$$

If we assume k_{reinit} for $\text{H}\bullet$ transfer from Cr hydride to MMA is equal to $k_{\text{C-H-Cr}}$ for $\text{H}\bullet$ transfer from Cr hydride to the vinyl-

terminated polymer **6**, eq 19 means that we can determine a true ΔG for Scheme 8 from $k_{tr}(\text{polymer})/k_{\text{reinit}}$. Our values of these rate constants at 50 °C give a ΔG of -13.5 kcal/mol in toluene. Neglecting ΔS and using our Cr–H BDE give 46.1 kcal/mol as the BDE at 50 °C for the C–H bond in **3-P**—to our knowledge the first determination of the strength of a C–H bond in the chain-carrying radical of a *polymerization* reaction.

Unfortunately, the BDE(C–H) that we have just calculated for **3-P** (46.1 kcal/mol) cannot be compared with the BDE(C–H) that we calculated earlier from our “experiment/theory hybrid” for **3** (45.6 kcal/mol), since the BDE for **3-P** neglected ΔS . It is better to compare ΔG for $\text{H}\bullet$ transfer to the polymer-substituted double bond in the vinyl-terminated polymer **6** (+13.5 kcal/mol), with the ΔG we obtained (from k_{reinit} and k_{tr} without allowing for cage effects) for $\text{H}\bullet$ transfer to MMA (eq 17) (+11.4 kcal/mol). The fact that ΔG is larger for $\text{H}\bullet$ transfer to the polymer-substituted double bond suggests that the C–H BDE in **3-P** is lower than that in **3** itself, which is not unreasonable: **3** and **3-P** differ in the number of equivalent C–H bonds by a factor of 2, and the C–H bond strength may be influenced by the substituent effect of the polymer chain. We have explored the latter possibility by calculating (at the suggestion of a reviewer) the gas-phase BDE for the “mono-substituted” radical **7** (**3** + MMA); the results (Table S10) indicate that the C–H bond in **7** is indeed 0.8 kcal/mol weaker. (Although we have calculated entropy corrections for **7**, they are unlikely to be good approximations for the polymer-substituted radical **3-P**.)



It is also possible that our ΔG for $\text{H}\bullet$ transfer to the vinyl-terminated polymer **6** (+13.5 kcal/mol) differs from our ΔG for $\text{H}\bullet$ transfer to MMA (+11.4 kcal/mol) because our kinetic analysis of the latter situation (eq 17) did not include cage effects.

Experimental Section

General. All manipulations were carried out using Schlenk, high-vacuum, or inert-atmosphere-box techniques, unless otherwise indicated. THF, C_6D_6 , and toluene- d_8 were distilled under

- (42) Jacobsen, E. N.; Bergman, R. G. *J. Am. Chem. Soc.* **1985**, *107*, 2023–2032.
- (43) Tang, L.; Norton, J. R. in preparation, to be submitted to *Macromolecules*.
- (44) A similar “negative activation energy” has been seen, and a similar explanation (reversible formation of a dissociable intermediate) offered, for a carbene/alkene cycloaddition in Turro, N. J.; Lehr, G. F.; Butcher, J. A., Jr.; Moss, R. A.; Guo, W. *J. Am. Chem. Soc.* **1982**, *104*, 1754–1756.
- (45) The bond between the sterically encumbered ($\eta^5\text{-C}_5\text{Ph}_5$)Cr(CO)₃• (**1a**) and the tertiary radical **3-P** will be weak. Formation of such a bond would reduce the efficiency of **1a** as a chain transfer catalyst,⁴⁶ as the resulting alkyl complex **5** cannot be an intermediate in formation of the hydride **2a** (**5** would have no vacant coordination site and thus be unable to undergo β -hydrogen elimination).⁴⁷ Weak interaction between the metalloradical **1a** and the carbon-centered radical **3-P** can, however, contribute to the formation of the cage in Scheme 6.
- (46) Reversible formation of a Co–C bond has been observed with Co(II) chain transfer catalysts and the α -methylbenzyl radical **4** in styrene polymerization, but it is insignificant with the isobutryl radical **3** in MMA polymerization. Heuts, J. P. A.; Forster, D. J.; Davis, T. P. *Macromolecules* **1999**, *32*, 2511–2519.
- (47) Similarly, the release of alkenes from alkyl cobalamins occurs not by β -hydrogen elimination but by $\text{C} \rightarrow \text{Co H}\bullet$ transfer after homolysis of the Co–C bond. See Halpern, J. *Pure Appl. Chem.* **1979**, *51*, 2171, and Bonhôte, P.; Scheffold, R. *Helv. Chim. Acta* **1991**, *74*, 1425–1444.

N₂ from Na/benzophenone. Et₂O, hexanes, CH₂Cl₂, benzene, and toluene were degassed and passed through columns of activated alumina and supported copper catalyst.⁴⁸

Materials. Styrene was washed 3 times with 5% NaOH and NaCl solutions to remove inhibitors. It was dried over CaH₂, distilled under reduced pressure, and stored in the freezer at −30 °C. It was then distilled immediately prior to use.

Methyl methacrylate was predried over MgSO₄, and then ran down an Aldrich Inhibitor Removal Column to remove inhibitor. It was vacuum-transferred over CaH₂, stored at −30 °C, and vacuum-transferred immediately prior to use.

MMA-*d*₅ and styrene-*d*₈ were purchased from Aldrich in sealed ampules. The inhibitor was removed from the MMA-*d*₅ by vacuum-transfer from CaH₂, and from the styrene-*d*₈ by vacuum-transfer alone.

(η^5 -C₅Ph₅)Cr(CO)₃• (**1a**),³ (η^5 -C₅Ph₅)Cr(CO)₃H⁴ (**2a**), (η^5 -C₅Me₅)Cr(CO)₃H (**2b**),⁴⁹ and (η^5 -C₅H₅)Cr(CO)₃H (**2c**)⁵⁰ were prepared by literature procedures. AIBN was recrystallized by methanol twice and stored at −35 °C. Hexamethylcyclotrisiloxane was purified by vacuum-transfer. Bis(triphenylphosphine)iminium cyclopentadienyl chromium tricarbonyl ([PPN]-[CpCr(CO)₃]) was synthesized according to a published procedure for the molybdenum species.⁵¹

Measurement of the Extinction Coefficient of (η^5 -C₅Ph₅)-Cr(CO)₃• (1a**) in Toluene** is described in the Supporting Information.

NMR Kinetic Measurements. Rate Law for H• Transfer from (η^5 -C₅Ph₅)Cr(CO)₃H (2a**) to MMA.** All NMR kinetic measurements were recorded on a 300 MHz instrument. In a typical experiment, a C₆D₆ solution (300 μ L) of **2a** (0.030 M) and hexamethylcyclotrisiloxane (as an internal standard) (0.002 M) was placed in a J. Young NMR tube. A C₆D₆ solution (300 μ L) of 2.00 M MMA-*d*₅ was added to the same tube and frozen in liquid N₂. The tube was placed in the NMR probe (equilibrated to a temperature calibrated by ethylene glycol⁵² as 323.0 \pm 0.5 K, and already tuned with a similar tube) and allowed to thaw. The extent of reaction was determined by monitoring the decrease in the peak height (related to the internal standard) of the hydride resonance (δ −3.98). The time-dependent hydride concentrations were fitted to eq 4, 5, 6 with KaleidaGraph; both [CrH] _{∞} and *k*_{obs} were refined. A plot of *k*_{obs} vs [MMA-*d*₅] is shown as Figure S2

$$[\text{CrH}]_t = [\text{CrH}]_{\infty} + ([\text{CrH}]_0 - [\text{CrH}]_{\infty})e^{-k_{\text{obs}}t} \quad (20)$$

Rate Constants *k*_{reinit} for H• Transfer from (η^5 -C₅R₅)Cr(CO)₃H (R = Ph, Me, H) (2a,b,c**) to MMA-*d*₅ and Styrene-*d*₈.** The same general procedure as in the previous paragraph was followed with MMA-*d*₅. To obtain activation parameters, *k*_{reinit} from **2a** to MMA-*d*₅ was measured from 333 K to 308 K (Table S2). Similarly, the kinetics of H• transfer from **2b** to MMA-*d*₅ were observed from 323 K to 303 K in C₆D₆ (Table S3). Lower temperatures were needed to obtain accurate kinetic

data for H/D exchange between **2c**⁵³ and MMA-*d*₅, so toluene-*d*₈ was used as a solvent instead of benzene; the rate constants obtained from 308 K to 288 K are given in Table S4.

With styrene-*d*₈ modification was required because the reaction was considerably faster. The solution of **2** with the internal standard was placed in an NMR tube and frozen inside an inert atmosphere box, the styrene-*d*₈ solution was added by syringe, and the tube was immediately put back in the freezer of the inert atmosphere box. The tube was flame-sealed while frozen. The solution was thawed and mixed just before it was placed in the NMR probe.

The rate constants for styrene-*d*₈ and (η^5 -C₅Ph₅)Cr(CO)₃H (**2a**), (η^5 -C₅Me₅)Cr(CO)₃H (**2b**), are shown in Table S5, S6; the rate constants for styrene hydrogenation with (η^5 -C₅H₅)Cr(CO)₃H (**2c**) are shown in Table S7.

Determination of the Rate Constants *k*_{tr} for H• Transfer to (η^5 -C₅Ph₅)Cr(CO)₃• (1a**) from the methyl isobutyryl radical **3** and α -methyl benzyl radical **4**.** Solutions of (η^5 -C₅Ph₅)Cr(CO)₃H (**2a**) and MMA or styrene in toluene (see Table 4) were made in an inert atmosphere box and placed in a UV cell (quartz, 1 cm path length) that could be attached to a Schlenk line with a Teflon stopcock. The cell, filled with an inert atmosphere, was detached from the Schlenk line and placed in the Peltier temperature controller (previously equilibrated to the desired temperature) inside the UV spectrometer. Absorbance data at 611 nm were collected every 30s for the first h; thereafter, the time between spectra was incremented by 10% on each scan. The reaction was complete after 20 h.

The value of *k*_{tr} was obtained using MacKinetics¹⁵ simulation software, with initial concentrations for all species and the time dependence of the chromium radical **1a** (calculated from the absorbance data with ϵ = 720 M^{−1}cm^{−1}) as input. The rate constants *k*_{reinit} = 0.0017 M^{−1}s^{−1} (for methyl isobutyryl radical **3**, from Table 1) and 0.018 (for α -methyl benzyl radical **4**, from Table 3) and *k*_{term} = 1.65 \times 10⁸ M^{−1}s^{−1} (for **3**)^{13,14} and 3.2 \times 10⁷ M^{−1}s^{−1} (for **4**)¹⁶ were fixed and *k*_{tr} determined by iteration. The results for MMA are in Table 4.

Determination of the *pK*_a of (η^5 -C₅Ph₅)Cr(CO)₃H (2a**)** A typical experiment is described. Two 1 mL solutions of [PPN]-[CpCr(CO)₃] (23.5 mg) and **2a** (15.2 mg) in CD₂Cl₂ were prepared. A weighed aliquot from each solution was measured into an NMR tube with a resealable Teflon stopcock to give a final volume of approximately 1 mL. Spectra were taken between 230 and 270 K, and the Cp resonances of CpCr(CO)₃H and CpCr(CO)₃• were integrated. From the known initial amounts of **2a** and [PPN][CpCr(CO)₃] and the ratios of the Cp resonances the equilibrium constant for proton exchange was calculated. Four NMR equilibrium measurements yielded a *pK*_a of 11.7(3).

Computational Details. All calculations were carried out using the Jaguar 4.1 suite⁵⁴ of ab initio programs. The geometries

(48) Pangborn, A. B.; Giardello, M. A.; Grubbs, R. H.; Rosen, R. K.; Timmers, F. J. *Organometallics* **1996**, *15*, 1518.

(49) Leoni, P.; Landi, A.; Pasquali, M. J. *Organomet. Chem.* **1987**, *321*, 365.

(50) Keppie, S. A.; Lappert, M. F. J. *Organomet. Chem.* **1969**, *19*, P5.

(51) Darensbourg, M. Y.; Jimenez, P.; Sackett, J. R.; Kanckel, J. M.; Kump, R. L. *J. Am. Chem. Soc.* **1982**, *104*, 1521–1530.

(52) Cavanagh, J.; Fairbrother, W. J.; Palmer, A. G., III; Skelton, N. J. *Protein NMR Spectroscopy Principles and Practice*; Academic Press New York, 1996.

(53) During the ¹H/²D exchange experiments between excess MMA-*d*₅ and the hydride complex **2c** (η^5 -C₅H₅)Cr(CO)₃H, the ¹H NMR resonance of the Cp of **2c** broadened and shifted downfield (to δ 5.2 at the end of the experiment), although that of the hydride remained sharp. The extent of the broadening varies from experiment to experiment. It appears to arise from fast H• exchange between CpCr(CO)₃H and traces of the metalloradical **1c** (CpCrCr(CO)₃•), present in equilibrium with its dimer [CpCr(CO)₃]₂. (It is difficult to avoid introducing traces of **1c** during the synthesis of **2c**, and some **1c** is formed in the course of the ¹H/²D exchange.)

(54) Jaguar 4.1, Schrödinger Inc, Portland, OR, 2000.

of all species were fully optimized using the B3LYP functional⁵⁵ and the 6-31G** basis set. Although this basis set is known to give reliable geometries, the energies are expected not to be sufficiently accurate, in particular for the radical species that require a high-quality basis. Therefore, we re-evaluated the energies using the correlation consistent triple- ζ basis⁵⁶ cc-pVTZ(-f)++ including two sets of diffuse functions in addition to the standard set of two polarization functions. The chromium atom was represented using the Los Alamos LACVP** basis,⁵⁷ which contains effective core potentials and corresponds to the 6-31G** basis used for all main-group elements, in geometry optimizations. For single point calculations, we used a modified version of LACVP**, denoted LACV3P**++, where the exponents were decontracted and diffuse functions were added to match the cc-pVTZ(-f)++ basis of the main group elements. All calculations made use of the unrestricted spin formalism. Cartesian coordinates of all optimized structures are given in Supporting Information.

Vibrational frequencies based on analytical second derivatives were computed at the B3LYP/6-31G** level of theory and unscaled frequencies were used to deduce vibrational zero-point energy (ZPE) corrections. For both chromium complexes this level of theory gave rise to a physically meaningless imaginary frequency at $\sim 40\text{ cm}^{-1}$ that was assigned to a rotation of the Cp-ring around an axis connecting the Cr center with the center of mass of the Cp-ring. Re-evaluation of the vibrational frequencies for both Cr-complexes at the B3LYP/cc-pVTZ(-f)/LACV3P** level of theory gave no imaginary frequency confirming the widely accepted practice of ignoring all imaginary frequencies below 100 cm^{-1} . The thermodynamic properties derived from these two levels of theory are practically identical for both cases and are given in the Supporting Information.

Solvation effects were taken into account using a continuum solvation model⁵⁸ by numerically solving the Poisson–Boltzmann equation.⁵⁹ Rather than reoptimizing the geometry with the self-consistent-reaction-field potential added to the Hamiltonian, we simply used the gas phase geometry and computed

the solvation energy in single point calculations at the B3LYP/6-31G**/LACVP** level of theory with the dielectric constant set to 2.379 and 37.5 to emulate toluene and acetonitrile, respectively. Basis set effects on solvation energy and the general performance of this protocol have been investigated explicitly elsewhere,⁶⁰ and found to be sufficiently small that a re-evaluation of the solvation energy at the cc-pVTZ(-f)++ level of theory is not necessary.

Bond Dissociation Energies. To compute the gas-phase bond dissociation enthalpy, $\Delta H(\text{gas})$, the vibrational zero-point energy difference (ΔZPE) and thermal corrections ΔH^T ($H^T = \int C_p dT$; C_p = heat capacity; T = temperature) have been added to the electronic bond dissociation energy ΔH^{SCF} : $\Delta H = \Delta H^{\text{SCF}} + \Delta ZPE + \Delta H^T + 5/2RT$. The electronic energy H^{SCF} is the single point energy computed at the B3LYP/cc-pVTZ(-f)++ level of theory. The electronic energy of $\text{H}\cdot$ at the B3LYP/cc-pVTZ(-f)++ level of theory is 13.667 eV. The last term ($5/2RT$) is the thermal correction for free $\text{H}\cdot$ and amounts to 1.48 kcal/mol at room temperature. ΔS , the entropy corrections in gas phase are derived using standard approximations of statistical mechanics. The translational entropy of free hydrogen is computed using the Sackur-Tetrode equation (26.04 eu). In evaluating the solution phase energies, it is desirable to obtain the enthalpy and entropy of solvation separately, which would allow for computing bond dissociation enthalpy and the free energy of bond dissociation in solution. However, continuum solvation models are by default unable to separate these terms and simply give the overall free energy of solvation. Thus $\Delta H(\text{sol})$ we list in Table 5 is $\Delta H(\text{sol}) = \Delta H(\text{gas}) + \Delta G(\text{solvation})$. Although the hybrid energy $\Delta H(\text{sol})$ is therefore rigorously not meaningful, it is a helpful one because it gives an estimate for the solvation corrected bond dissociation enthalpy. The solvation energy of $\text{H}\cdot$ is assumed to be the same as that of the H_2 molecule and set to +3.40 kcal/mol. We use the experimental solvation enthalpy ($\Delta H^{\text{Solv}} = 5.773\text{ kJ/mol}$) and entropy ($\Delta S^{\text{Solv}} = -47.68\text{ J/(mol K)}$) determined by Brunner¹⁹ for toluene ($\epsilon = 2.379$). Appropriate values for acetonitrile have been used accordingly (see the Supporting Information).

Acknowledgment. This work was supported by grants from the DOE to J.R.N. (DE-FG02-97ER14807) and from the NIH to R.A.F. (GM40526). The authors are grateful to Prof. N. Turro and A. Maliakal for helpful discussions.

Supporting Information Available: Measurement of extinction coefficient of $(\eta^5\text{-C}_5\text{Ph}_5\text{Cr}(\text{CO})_3)\cdot$, details of $(\eta^5\text{-C}_5\text{R}_5\text{Cr}(\text{CO})_3\text{H/MMA-}d_5$ and $(\eta^5\text{-C}_5\text{R}_5\text{Cr}(\text{CO})_3\text{H/styrene-}d_8$ isotope exchange, and details of DFT computation (PDF). This material is available free of charge via the Internet at <http://pubs.acs.org>.

JA034927L

- (55) (a) Becke, A. D. *J. Chem. Phys.* **1993**, *98*, 5648. (b) Lee, C. T.; Yang, W. T.; Parr, R. G. *Phys. Rev. B* **1988**, *37*, 785.
 (56) Dunning, T. H. *J. Chem. Phys.* **1985**, *89*, 4207.
 (57) Hay, P. J.; Wadt, W. R. *J. Chem. Phys.* **1985**, *82*, 270.
 (58) (a) Cramer, C. J.; Truhlar, D. G. *Structure and Reactivity in Aqueous Solution*, ACS Symposium Series 568; American Chemical Society: Washington, D. C., 1994. (b) Tomasi, J.; Persico, M. *Chem. Rev.* **1994**, *94*, 2027. (c) Patterson, E. V.; Cramer, C. J.; Truhlar, D. G. *J. Am. Chem. Soc.* **2001**, *123*, 2025.
 (59) (a) Friedrichs, M.; Zhou, R. H.; Edinger, S. R.; Friesner, R. A. *J. Phys. Chem. B* **1999**, *103*, 3057–3061. (b) Edinger, S. R.; Cortis, C.; Shenkin, P. S.; Friesner, R. A. *J. Phys. Chem. B* **1997**, *101*, 1190–1197. (c) Marten, B.; Kim, K.; Cortis, C.; Friesner, R. A.; Murphy, R. B.; Ringnalda, M. N.; Sitkoff, D.; Honig, B. *J. Phys. Chem.* **1996**, *100*, 11 775–11 788.
 (60) Baik, M.-H.; Friesner, R. A. *J. Phys. Chem. A* **2002**, *106*, 7407.